

# New Limits on Tau Neutrino Mass from CLEO II

Jon Urheim\*

*California Institute of Technology*

I report on two studies of tau neutrino mass recently carried out using data collected with the CLEO II detector at the CESR  $e^+e^-$  collider. First I present the results of an analysis of 473 decays of the type  $\tau^\pm \rightarrow \nu_\tau 5\pi^\pm$  and  $\tau^\pm \rightarrow \nu_\tau 3\pi^\pm 2\pi^0$ , from which a 95% CL upper limit on  $m_{\nu_\tau}$  of 30 MeV is obtained. Results are also presented from a preliminary analysis of the decay  $\tau^\pm \rightarrow \nu_\tau 3\pi^\pm \pi^0$ , using a sample of  $\sim 29,000$  reconstructed events. In addition, I report on a study of hadronic structure in  $\tau^\pm \rightarrow \nu_\tau \pi^\pm 2\pi^0$ , and discuss the implications for neutrino mass analyses based on the  $\nu_\tau 3\pi$  decay channel. Prospects for improved constraints on  $m_{\nu_\tau}$  in the near future are examined.

## I. INTRODUCTION

In this contribution, I discuss two recent efforts from the CLEO experiment on the question of  $\tau$  neutrino mass. The motivation for using  $\tau$  lepton decay to directly investigate possible  $\nu_\tau$  masses in the range 1–30 MeV was summarized by Cerutti [1] at this conference. It is worth reiterating that a  $\nu_\tau$  mass in this range is experimentally and cosmologically viable — that is, provided the observed deficits and asymmetries in atmospheric  $\nu_\mu$  fluxes [2–4] turn out to be attributable to phenomena other than  $\nu_\mu \leftrightarrow \nu_\tau$  oscillations.

As with the direct limits on masses of the other neutrino flavors, studies of  $m_{\nu_\tau}$  in  $\tau$  decay are difficult undertakings, and progress has been slow. See Refs. [1,5,6] for reviews of recent work in this area. These analyses require detailed understandings of many difficult experimental and theoretical issues, including backgrounds, detector response and resolution, and the dynamics of semi-hadronic  $\tau$  decays, as well as statistical issues.

In the next section, I describe the CLEO II detector and its suitability for  $\nu_\tau$  mass studies in light of some of the above issues. In Sec. III, I report on a recently published CLEO analysis [7] of  $\tau$  decays to  $\nu_\tau$  plus five pions. A preliminary analysis of the copious  $\tau$  decay  $\tau^\pm \rightarrow \nu_\tau 3\pi^\pm \pi^0$  is presented in Sec. IV. Finally, in Sec. V, I present results on hadronic structure in the  $\nu_\tau 3\pi$  decay channel, and discuss implications for  $\nu_\tau$  mass studies using this decay such as those recently carried out at LEP [1,6]. The talk closes with a discussion of future prospects in Sec. VI.

## II. THE CLEO II DETECTOR AND ASSOCIATED NEUTRINO MASS ISSUES

The CLEO experiment is carried out at the Cornell Electron Storage Ring (CESR) where  $\tau$ 's are produced in pairs via  $e^+e^- \rightarrow \tau^+\tau^-$  at center-of-mass energies of  $E_{cm} = 2E_{beam} \sim 10.6$  GeV. The main detector elements [8] are cylindrical tracking and calorimetric devices enclosed within a 1.5T superconducting solenoid. The calorimeter consists of 7800 CsI(Tl) crystals, presenting 16 radiation lengths to photons originating from the  $e^+e^-$  interaction point. The tracker consists of an inner detector surrounded by small-cell drift chambers comprising 10 and 51 anode layers. Between 1989 and 1995,  $5 \text{ fb}^{-1}$  of collision data was collected in the CLEO II configuration, in which the inner tracking detector was six layers of straw tubes. Between November 1995 and February 1999, an additional  $9 \text{ fb}^{-1}$  of data was acquired with the CLEO II.V detector, in which the straw tubes were replaced by a three-layer double-sided silicon microstrip detector. Later this year, the CLEO III detector will turn on with significantly upgraded tracking and particle identification capabilities. For the studies described here, we have analyzed only the CLEO II data.

As in the LEP analyses, CLEO makes use of the kinematic properties of semi-hadronic  $\tau$  decay, as depicted in Fig. 1. The invariant mass  $\sqrt{s} = M_X$  of the hadronic system  $X$  produced in such decays depends in part on the well-known weak decay dynamics and phase space factors, shown in the expression for a massless  $\nu_\tau$ . The top plot in

---

\*representing the CLEO Collaboration.

Fig. 2 shows the distributions associated with these factors for two values  $m_{\nu_\tau}$ . The  $M_X$  spectrum also depends on the spectral function  $v(s)$  for the particular decay mode being studied. This function does not depend on  $m_{\nu_\tau}$ , but rather on the (usually poorly known) strong interaction dynamics associated with the formation (via the hadronic weak current) and decay of the hadronic state. The bottom plot shows the spectral function inferred for the decay  $\tau^\pm \rightarrow \nu_\tau 3\pi^\pm \pi^0$ , one of the modes discussed here. The distribution in the energy  $E_X$  of the hadronic system also has sensitivity to  $m_{\nu_\tau}$ , particularly for events with large  $M_X$  (see Figs. 3 and 4). However, unlike the  $M_X$  spectrum itself, the  $E_X$  distribution within a small slice in  $M_X$  does not directly depend on the hadronic physics.

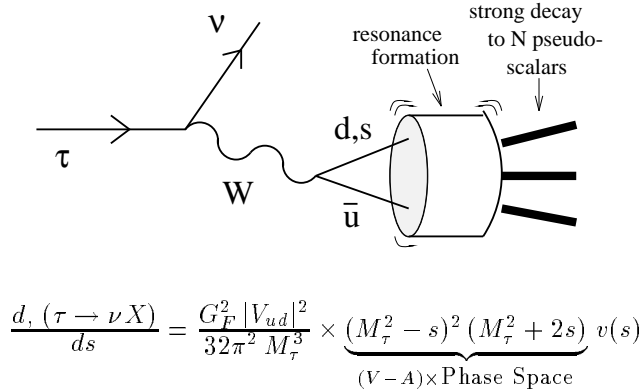


FIG. 1. Cartoon of semi-hadronic  $\tau$  lepton decay. The expression for  $d, (\tau \rightarrow \nu X)/ds$  assumes  $m_{\nu_\tau} = 0$ .

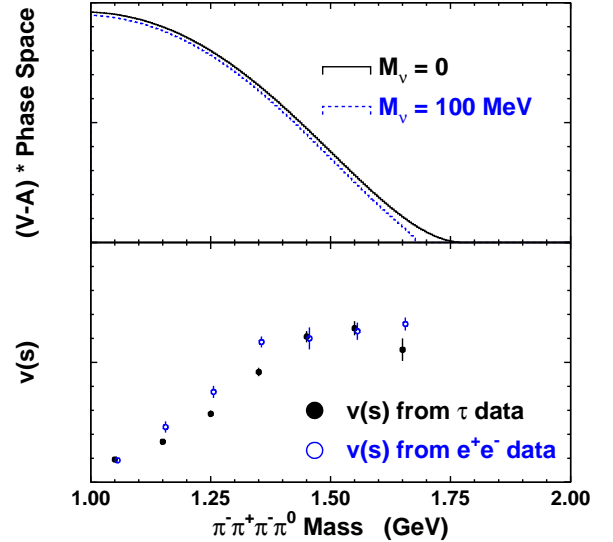


FIG. 2. Contributions to  $d, (\tau \rightarrow \nu_\tau X)/ds$ , for  $X = 3\pi^\pm \pi^0$ : weak decay and phase space factors (top), and the  $3\pi^\pm \pi^0$  spectral function (bottom) as inferred from  $\tau$  decay (filled points) and from  $e^+e^- \rightarrow 4\pi$  using CVC.

Like those discussed by the previous speaker [1], the two analyses presented here involve studies of both low-rate ( $\tau \rightarrow \nu_\tau 5\pi$ ) and high-rate ( $\tau \rightarrow \nu_\tau 4\pi$ ) decay channels. Also similar to the LEP analyses, the technique employed is an unbinned likelihood fit to the distribution of events in the kinematic observables sensitive to  $m_{\nu_\tau}$ , namely  $E_X$  and  $M_X$ . Those features unique to our analyses are discussed in the following sections.

Carrying out neutrino mass studies at CLEO has several advantages relative to the LEP experiments. First, with its record luminosity performance, CESR is the richest source of  $\tau$ -pair events: the  $5.0 \text{ fb}^{-1}$  of CLEO II data correspond to 4.5 million produced  $\tau$ -pairs, roughly 20 times the per experiment yield at LEP. Second, due to the lower beam energy, the  $\tau$  boost is smaller, resulting in larger separation of  $\tau$  decay particles in the detector. This leads to favorable conditions for pattern recognition, as well as smaller correlations between  $E_X$  and  $M_X$  than at LEP. Also, because  $\tau$  decay particles are well-separated, the segmentation and energy resolution of the calorimeter allows modes with  $\pi^0$ 's to be used for neutrino mass studies, unlike the situation at LEP.

However, the lower beam energy brings an important disadvantage: the mean charged particle multiplicity from hadronic ( $e^+e^- \rightarrow q\bar{q}$ ) events at  $E_{cm} = 10.6 \text{ GeV}$  is approximately 10 — half that at LEP. Thus, low-multiplicity hadronic events present a dangerous background for CLEO. To mitigate this background source, tight cuts must be applied, offsetting somewhat the advantage of high luminosity.

### III. ANALYSIS OF THE $5\pi$ MODES: $\nu_\tau 5\pi^\pm$ AND $\nu_\tau 3\pi^\pm 2\pi^0$

The  $5\pi$  analysis [7] makes use of the full CLEO II data set, representing 4.5 million produced  $\tau$ -pair events. This work supercedes a previous CLEO analysis [9] of a subset of this data. As in that analysis, we study two  $5\pi$  modes:  $\nu_\tau 5\pi^\pm$  and  $\nu_\tau 3\pi^\pm 2\pi^0$ , the latter exploiting the capabilities of the CsI calorimeter.

The analysis is driven by the features of these decay modes. First, they are rare, having branching fractions <sup>1</sup> of 0.08% and 0.54%. Consequently, this is a low-statistics analysis where the ‘best’ one or two events count the most in constraining  $m_{\nu_\tau}$ . Thus, even a single background event can spoil the measurement, leading to a spuriously stringent limit. To suppress  $q\bar{q}$  background, we require the decay of the  $\tau$  recoiling against the  $5\pi$  system to be consistent with  $\tau$  decay to  $e\bar{\nu}\nu$  or  $\mu\bar{\nu}\nu$ . We require the momentum sum of the reconstructed particles in each event to be non-zero so as to be consistent with the presence of neutrinos. We also apply tight cuts on extraneous activity in the calorimeter to veto hadronic events in which the ‘missing’ momentum is carried by photons or showering neutrons or  $K_L$ ’s. Finally, to account for residual backgrounds, we include an explicit background term in our likelihood function (see below).

The second feature concerns the dynamics underlying the production of the  $5\pi$  system. From conservation of parity and  $G$ -parity, we know this system is predominantly axial vector ( $J^P = 1^+$ ). Unfortunately, the properties of light axial vector mesons are not well measured (see Sec. V). This feature motivates us to include in our fit only those events lying within a small region near the  $M_X$  endpoint, illustrated in Fig. 3. Unlike the well-understood weak decay dynamics and phase space factors which are sensitive to  $m_{\nu_\tau}$ , the spectral function describing the (possibly resonant) line shape of the  $5\pi$  system is not expected to vary rapidly across this region.

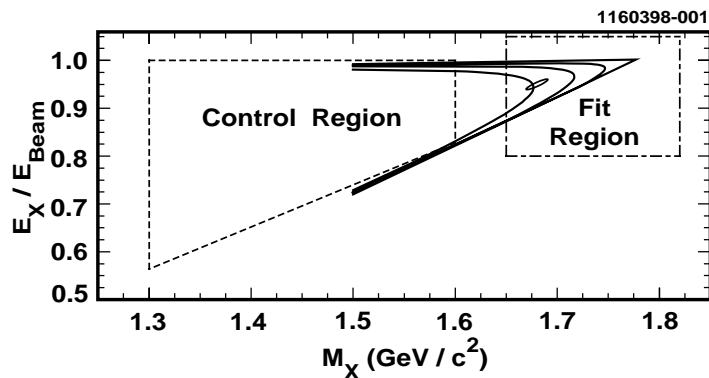


FIG. 3. Illustration of the portions of the space in  $E_X/E_{\text{beam}}$  and  $M_X$  used in the fit to the  $5\pi$  data samples. The curves represent the kinematic boundaries corresponding to different values of  $m_{\nu_\tau}$ .

The  $M_X$  distributions for the  $5\pi^\pm$  and  $3\pi^\pm 2\pi^0$  event samples are plotted in Figs. 4(a) and (b). There are 258 (196) events below  $m_\tau$  and 8 (13) events above  $m_\tau$  in the two samples, respectively. Based on the number of events above  $m_\tau$  and an empirically-determined  $q\bar{q}$  background shape, we estimate that  $0.3 \pm 0.1$  and  $0.4 \pm 0.1$   $q\bar{q}$  events enter the fit regions in the two samples. The scatter plots in  $E_X/E_{\text{beam}}$  versus  $M_X$  are shown for the fit region only in Figs. 4(c) and (d). There are 36 events in  $5\pi^\pm$  sample and 19 events in the  $3\pi^\pm 2\pi^0$  sample in this region.

<sup>1</sup>The  $\nu_\tau 3\pi^\pm 2\pi^0$  rate is enhanced by the presence of a large  $\nu_\tau \pi^\pm \omega \pi^0$  component.

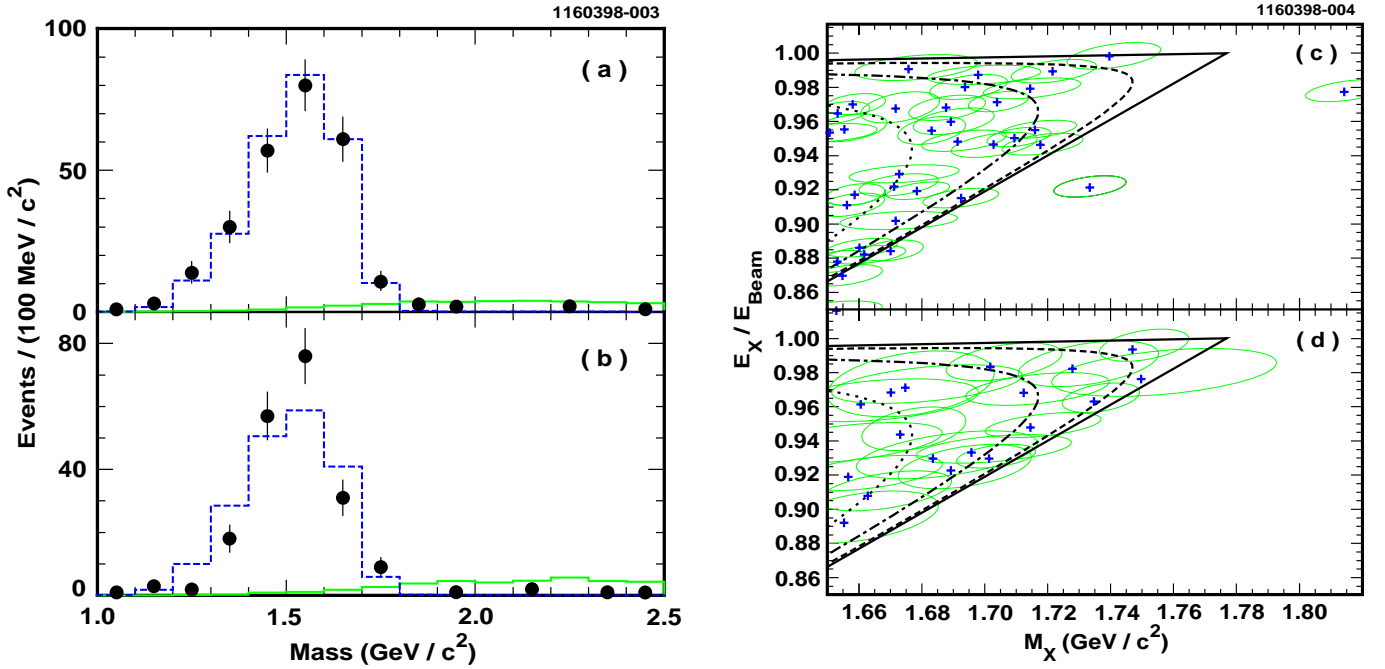


FIG. 4. (a) and (b): the  $5\pi$  invariant mass spectra for  $\nu_\tau 5\pi^\pm$  and  $\nu_\tau 3\pi^\pm 2\pi^0$  decay modes, respectively, from data (points) and  $\tau$  Monte Carlo (dashed) samples. Also shown are the expected  $q\bar{q}$  background distributions (dotted), scaled up by a factor of five for clarity. (c) and (d): the distribution of events (crosses) in the region of the  $E_{5\pi}/E_{\text{beam}}$  versus  $M_{5\pi}$  plane considered in the likelihood fit from the  $\nu_\tau 5\pi^\pm$  and  $\nu_\tau 3\pi^\pm 2\pi^0$  data samples. The curves denote kinematically allowed boundaries for  $m_{\nu_\tau} = 0, 30, 60$  and  $100$  MeV, ignoring initial state radiation. The 68% CL resolution contours derived from track and photon parameter errors are shown as ellipses surrounding the data points.

We perform an unbinned extended likelihood fit to the data where the likelihood function

$$\mathcal{L}(m_\nu) = \mathcal{P}(N_{\text{obs}}, m_\nu) \prod_i \left[ \alpha \mathcal{L}_{\text{Signal}}(\tilde{X}_i, \tilde{\sigma}_i, m_\nu) + (1 - \alpha) \mathcal{L}_{\text{Bkgnd}}(\tilde{X}_i, \tilde{\sigma}_i) \right], \quad (1)$$

depends on one unknown quantity,  $m_\nu$ , and is comprised of four elements:

- a signal function  $\mathcal{L}_{\text{Signal}}$  derived from the differential decay distribution in the kinematic observables for each event  $i$ ,  $\tilde{X}_i = (M_i, E_i/E_{\text{beam}})$ .
- a background function  $\mathcal{L}_{\text{Bkgnd}}$  in the same variables, based on Monte Carlo distributions for backgrounds from  $\tau$  decay modes other than the signal modes and on an independent  $q\bar{q}$ -enriched data sample for non- $\tau$  backgrounds. The quantity  $(1 - \alpha)$  above represents the overall background fraction.
- a Poisson factor  $\mathcal{P}$  parametrizing the dependence on  $m_\nu$  of the number of events entering the fit region as extrapolated from the number entering the control region (see Fig. 3).
- effective convolution of experimental resolution functions, denoted as  $\tilde{\sigma}_i$  in the above expression. These are derived by propagating individual event track and photon error matrices. Studies of  $D$  meson decays to  $K\pi$ ,  $K\pi\pi$ , and  $K3\pi$  as well as hadronic  $B$  meson decays are used to calibrate these resolutions, including tails.

This analysis is the first  $m_{\nu_\tau}$  analysis to make use of a Poisson factor or a background function in the likelihood formulation. The  $5\pi$  spectral function enters both signal likelihood and Poisson functions. We employ a model that uses input from  $e^+e^- \rightarrow 4\pi$  and  $6\pi$  data, and is tuned (ignoring the mass endpoint region) to an independent sample of  $\tau \rightarrow \nu_\tau 5\pi$  events in which the recoiling  $\tau$  decays to  $\nu_\tau \pi$ . The Poisson factor makes use of some of the information from events outside of the fit region, but does not depend as strongly on the details of the model for the spectral function as would an approach employing a larger fit region. From toy Monte Carlo simulations, we find that including this factor improves the reliability of interpreting the likelihood function as a probability distribution.

The raw likelihood values are plotted as a function of  $m_{\nu_\tau}$  for the  $5\pi^\pm$ ,  $3\pi^\pm 2\pi^0$  and combined samples in Fig. 5. The results are consistent with the hypothesis of a massless neutrino. The combined likelihood is integrated to yield a 95% CL upper limit on  $m_{\nu_\tau}$  of 27 MeV, not including systematic errors.

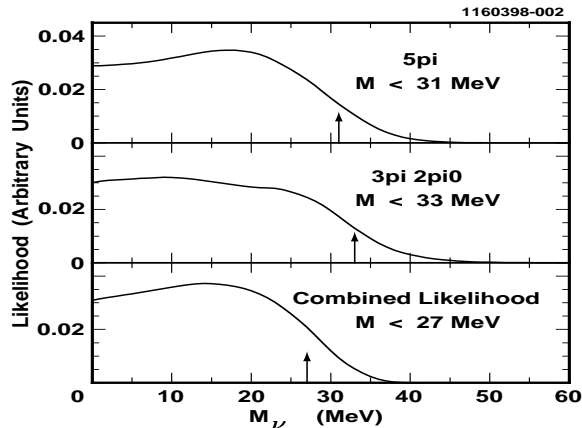


FIG. 5. The raw likelihood distributions for  $\nu_\tau 5\pi^\pm$ ,  $\nu_\tau 3\pi^\pm 2\pi^0$  and combined samples as a function of  $\nu_\tau$  mass. Systematic errors are not included.

Systematic errors are evaluated using a procedure similar to that employed by the LEP experiments [1]. The overall error is 3.1 MeV, bringing the 95% CL upper limit on  $m_{\nu_\tau}$  from the  $5\pi$  analysis to 30 MeV. The individual contributions to the systematic error are listed in Table I.

The limit obtained in this analysis, 31 MeV, compares poorly with the corresponding limit of 23.1 MeV obtained by ALEPH [10], especially considering that the sample used in the CLEO analysis is nearly ten times larger than that used by ALEPH. How can this be explained? Direct comparison of the  $M_{5\pi}$  spectra shows general agreement between the two experiments (as well as with the OPAL data [11]). However, ALEPH observes seven events with  $M_{5\pi}$  within 100 MeV of  $m_\tau$ , whereas 3.5 events would be expected based on the CLEO spectrum. The implication is that CLEO was less ‘lucky’ than ALEPH. From an ensemble of Monte Carlo experiments based on the spectral function used in the CLEO analysis, a more stringent limit than the one obtained by CLEO is expected in 2/3 of experiments with similar statistics. Thus, we conclude that although we were not particularly lucky, we were not especially unlucky either.

#### IV. ANALYSIS OF $\tau^\pm \rightarrow \nu_\tau 3\pi^\pm \pi^0$ DECAYS

The second analysis [12], involving reconstruction of  $\tau^\pm \rightarrow \nu_\tau 3\pi^\pm \pi^0$  decays, is the first use of this decay mode for  $m_{\nu_\tau}$  studies. Unlike the  $5\pi$  channels, the branching fraction is large,  $\sim 4.2\%$ . The spectral function for this channel, though still not well known, is in principle easier to model since the Conserved Vector Current theorem (CVC) provides a direct correspondence with  $e^+e^- \rightarrow 4\pi$  data (see Fig. 2). Also in contrast with the  $5\pi$  channel, the  $4\pi$  mass spectrum is concentrated below the endpoint region: like the analyses of  $\tau \rightarrow \nu_\tau 3\pi$  at LEP [1], the distribution in  $E_X$  plays a more significant role than that in  $M_X$  in constraining  $m_{\nu_\tau}$ . Fortunately, the  $4\pi$  mass spectrum is weighted more heavily towards the endpoint than the  $3\pi$  mass spectrum, thanks to the flatness of the spectral function (see Fig. 2) at high mass. This feature helps accentuate the sensitivity of the  $E_X$  distribution to non-zero values of  $m_{\nu_\tau}$ .

Although  $q\bar{q}$  backgrounds are proportionately larger in the  $4\pi$  final state, the high-statistics nature of the analysis renders it unlikely that a single background event will strongly influence the result. Consequently, we select events in which the recoiling  $\tau$  may decay to neutrino(s) plus  $e$ ,  $\mu$ ,  $\pi$ , or  $\pi\pi^0$ , comprising more than 70% of  $\tau$  decays. The

TABLE I. Systematic errors on the 95% CL  $m_{\nu_\tau}$  limits from the  $5\pi$  and  $4\pi$  analyses. Some error definitions differ slightly between the two analyses.

Source	Errors in MeV	
	5 $\pi$ Analysis	4 $\pi$ Analysis
Spectral Function	1.9	1.2
Mass/Momentum Scale	1.5	2.3
Energy Scale	0.2	3.7
Resolution Smearing	1.5	0.4
Background Normalization	0.3	0.8
MC Statistics	0.4	0.5
Total	3.1	5.1

resulting sample contains 29,000 events. The  $E_X$  versus  $M_X$  scatter plot for this sample is shown in Fig. 6(a). Also shown is the boundary delineating the fit region for this analysis. This region is larger than in the  $5\pi$  analysis, reflecting the lesser dependence on backgrounds and hadronic dynamics. There are 17,000 events in the fit region, of which 3% are  $q\bar{q}$  events and 7% are attributable to  $\tau$  decays to other final states.

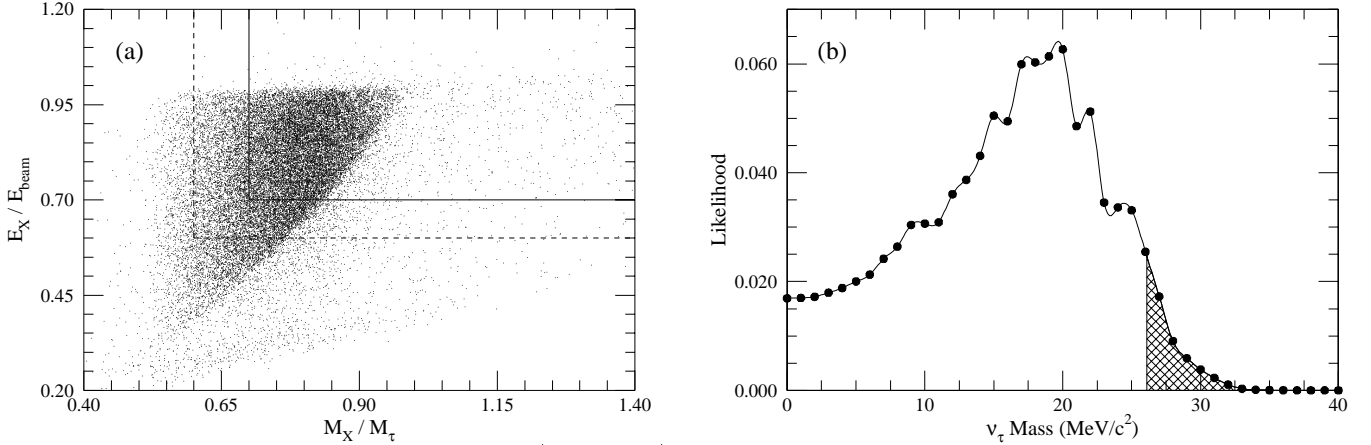


FIG. 6. (a) scatter plot of events from the  $\tau^\pm \rightarrow \nu_\tau 3\pi^\pm \pi^0$  sample in the  $E_{4\pi}/E_{\text{beam}}$  versus  $M_{4\pi}/m_\tau$  plane. The solid (dashed) lines delineate the nominal (alternate) region included in the likelihood fit. (b) The raw likelihood distribution for the  $\nu_\tau 3\pi^\pm \pi^0$  sample as a function of  $\nu_\tau$  mass. Systematic errors are not included.

The likelihood analysis proceeds as in the  $5\pi$  analysis, except that the large size of the fit region obviates the need for a Poisson factor. The raw likelihood curve is shown in Fig. 6(b), where integration to 95% of the area yields an upper limit of 26 MeV. Including the systematic errors given in Table I brings the limit to 31 MeV. Although the likelihood curve peaks away from zero, the likelihood for a zero-mass neutrino is sufficiently high that this curve should not be interpreted as an indication for a massive  $\nu_\tau$ . This analysis is preliminary. Additional work, including refinement of the spectral function model used in the likelihood fit, is in progress, but is not expected to result in a significant change in the limit.

## V. HADRONIC STRUCTURE IN THE DECAY $\tau^\pm \rightarrow \nu_\tau [3\pi]^\pm$

As reported by the previous speaker [1], competitive upper limits on  $m_{\nu_\tau}$  have been obtained by ALEPH, OPAL and DELPHI from analysis of the  $\tau^\pm \rightarrow \nu_\tau \pi^\pm \pi^+ \pi^-$  decay mode. Like the  $4\pi$  channel just discussed, this mode has a large branching fraction (9.2%), compensating for the fact that only a small fraction of events will lie in the sensitive region in  $E_X$  versus  $M_X$ . Unlike the  $4\pi$  analysis however, the  $3\pi$  spectral function is falling rapidly at high mass, by virtue of being on the tail of the poorly-understood  $a_1(1260)$  resonance that dominates this decay.

Might uncertainties in the hadronic dynamics in this decay pose a problem for  $m_{\nu_\tau}$  analyses? Although many models exist for this decay, none have been able to provide a satisfactory description of the  $3\pi$  mass spectra or the Dalitz plot distributions seen in data. This includes the spectral function models used by the LEP  $m_{\nu_\tau}$  analyses.

We have recently completed a detailed model-dependent analysis of hadronic structure in the decay  $\tau^\pm \rightarrow \nu_\tau \pi^\pm 2\pi^0$  [13]. The goal of this analysis was to characterize both the  $3\pi$  mass spectrum and the Dalitz plot distributions in a phenomenological context. We also wanted to shed light on the discrepancies between data and simple models of this decay, such as those apparent in the LEP  $m_{\nu_\tau}$  analyses. In our analysis we assume  $m_{\nu_\tau} = 0$ .

The distribution in  $M_{3\pi}$  for 31,000  $\tau^\pm \rightarrow \nu_\tau \pi^\pm 2\pi^0$  events (after subtraction of backgrounds) is shown in Fig. 7(a). The function shown is a fit to a single  $a_1(1260)$  Breit-Wigner using a mass dependent width,  $\Gamma_{tot}(s)$  illustrated in Fig. 7(b).

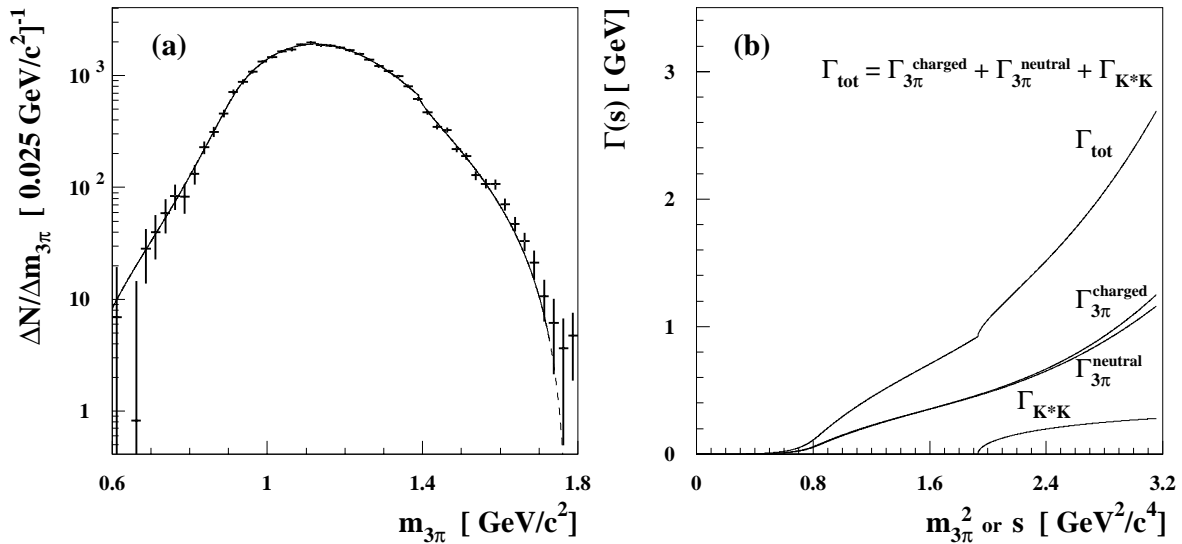


FIG. 7. (a) Acceptance-corrected, background-subtracted  $3\pi$  mass spectrum (points) from the CLEO  $\tau^\pm \rightarrow \nu_\tau \pi^\pm 2\pi^0$  sample. Overlaid is the  $a_1(1260)$  line shape fit function, assuming  $m_{\nu_\tau} = 0$  and no  $a_1'(1700)$  contribution. (b) Illustration of the mass-dependence of the total decay width of the  $a_1$  entering the Breit-Wigner parametrization used in (a). Also shown individually are the partial widths for  $3\pi^\pm$ ,  $\pi^\pm 2\pi^0$  and  $K^*K$  decay channels. The overall coupling for the  $K^*K$  mode is left as a free parameter in the fit in (a).

The form for  ${}_{tot}^{a_1}(s)$  is derived from a fit to the Dalitz plot distributions for resonant substructure contributions. Prior to this analysis, the  $a_1$  was believed to decay almost exclusively to  $\rho\pi$ . Our Dalitz plot fits demonstrated additional large contributions from substructure involving isoscalar mesons,  $\sigma\pi$ ,  $f_0(1370)\pi$  and  $f_2(1270)\pi$ , which together account for more than 25% of the  $a_1 \rightarrow 3\pi$  decay width. Inclusion of these amplitudes strongly affects the shape of  ${}_{tot}^{a_1}(s)$ , particularly at large  $s$ . We also included in  ${}_{tot}^{a_1}(s)$  a contribution from the turn-on of  $a_1 \rightarrow K^*K$  decay. This contribution is necessary in order to explain the apparent kink in the  $M_{3\pi}$  spectrum just below 1.4 GeV.

The analysis of DELPHI [14] suggested that a contribution from an  $a_1'(1700)$  was needed to account for an excess of events at high  $3\pi$  mass in their data. ALEPH [1] does not see indications for such a contribution. In the CLEO spectrum, there is clearly an excess above 1.575 GeV — this excess can be accounted for by an  $a_1$ , though at a level substantially below that observed by DELPHI. However, neither DELPHI nor ALEPH take into account the  $K^*K$  threshold, nor do they take into account the large increase in  ${}_{3\pi}^{a_1}(s)$  at high mass coming from the isoscalar channels. Both of these effects as well as the  $a_1'$  are crucial ingredients to a successful description of the  $M_{3\pi}$  spectrum. The effect of these distortions on  $m_{\nu_\tau}$  mass analyses is mitigated by the fact that the bulk of the sensitivity is in the  $E_X$  distribution. However, the credibility of  $\nu_\tau$  mass constraints based this mode will be greater once these effects are properly taken into account.

## VI. SUMMARY AND FUTURE OUTLOOK

To summarize, CLEO has carried out two analyses of  $\nu_\tau$ , based on  $\tau$  decays to final states containing four and five pions in the CLEO II data sample corresponding to 4.5 million  $\tau$ -pair events. The raw 95% CL upper limits on  $m_{\nu_\tau}$  are 27 MeV and 26 MeV from the  $\nu_\tau 5\pi$  and  $\nu_\tau 4\pi$  samples, respectively. Including systematic errors, the limits are:

$$m_{\nu_\tau} < 30 \text{ MeV}, \quad \nu_\tau 5\pi^\pm / 3\pi^\pm 2\pi^0 \text{ channels}, \quad (2)$$

$$m_{\nu_\tau} < 31 \text{ MeV}, \quad \nu_\tau 3\pi^\pm \pi^0 \text{ channel (preliminary)}. \quad (3)$$

Additional work finalizing the  $3\pi^\pm \pi^0$  analysis, and on the careful combining of the limits from the two analyses should be completed in the near future. Although not as stringent as those from ALEPH, these limits are consistent with our expected sensitivity given the present statistics. In this sense, they are quite believable results.

Also, in a study of hadronic structure in  $\tau$  decay to final states containing three pions, we have characterized features in the Dalitz plot and  $3\pi$  mass distributions that are not well described by the simple models so far used in  $\nu_\tau$  mass analyses. This work should benefit future attempts to constrain  $m_{\nu_\tau}$  using this decay mode.

Since LEP running at the  $Z^0$  pole ended in 1995, CLEO is the only experiment that has continued to collect large samples of  $\tau$ -pairs. The CLEO II.V data represents an additional 8 million  $\tau$ -pair events, nearly tripling the total sample. In addition, the silicon detector and the use of He-based gas in the main drift chamber lead to improved resolutions, by a factor of 10% or so relative to CLEO II.

Later this summer, the CLEO III detector will commence data-taking after significant detector and accelerator upgrades. This detector features new tracking elements plus a fast RICH for enhanced  $K/\pi$  separation. Samples of 10–15 million  $\tau$ -pairs per year are expected. The improved particle ID capabilities will permit use of decays with charged kaons, such as  $\tau^\pm \rightarrow \nu_\tau K^+ K^- \pi^\pm$ , which are attractive for  $m_{\nu_\tau}$  studies by virtue of the small  $Q$ -value in these decays. High-quality, high-statistics samples are also expected from the asymmetric  $B$ -factory experiments BABAR and BELLE.

With the CLEO II.V data and the imminence of the  $B$ -factory era, there is good reason to hope for a new reach in sensitivity to  $m_{\nu_\tau}$ . However, some wariness is merited. As limits from individual measurements improve into the sub-20 MeV region, the difficulty of improving them further scales with an unknown but surely unfavorable dependence on statistics. Invariant mass resolutions of 10–20 MeV may soon become a limiting factor — a detailed understanding of resolution tails is already critical to the CLEO and LEP  $\nu_\tau$  mass measurements. Since the dependence on  $m_{\nu_\tau}$  in the distribution in  $E_X$  is quadratic, both momentum scale and resolution uncertainties are likely to limit sensitivity in this direction in the near future. All things considered, we should expect improvements in constraints on  $m_{\nu_\tau}$  in coming years, but these will not be obtained easily!

## VII. ACKNOWLEDGEMENTS

The CLEO Collaboration acknowledges the effort of the CESR staff in providing us with excellent luminosity and running conditions. I would like to thank Jean Duboscq for useful discussions, and acknowledge him and David Crowcroft for their work on the neutrino mass analyses described here. Moritz Schmidtler carried out the bulk of the  $3\pi$  structure analysis: he and Alan Weinstein are acknowledged for their contributions to that work.

- [1] F. Cerutti, these proceedings, Talk # 2-01.
- [2] Y. Fukuda *et al.* (Super-Kamiokande Collaboration), Phys. Rev. Lett. **81**, 1562 (1998); see also contributions from M. Messier and A. Habig, these proceedings, Talks 2-06 and 2-07.
- [3] M. Goodman, these proceedings, Talk # 2-08.
- [4] N. Longley and B. Nolty, these proceedings, Talks 2-09 and 2-10.
- [5] L. Passalacqua, Nucl. Phys. B (Proc. Suppl.) **55C**, 435 (1997).
- [6] R. McNulty, to appear in Proceedings of the Fifth Workshop on Tau Lepton Physics, Santander, Spain, September 1998, <http://www.ifca.unican.es/tau98>.
- [7] R. Ammar *et al.* (CLEO Collaboration), Phys. Lett. B **431**, 209 (1998).
- [8] Y. Kubota *et al.* (CLEO Collaboration), Nucl. Inst. Meth. **A320**, 66 (1992).
- [9] D. Cinabro *et al.* (CLEO Collaboration), Phys. Rev. Lett. **70**, 3700 (1993).
- [10] R. Barate *et al.* (ALEPH Collaboration), E. Phys. J. **C2**, 395 (1998).
- [11] K. Ackerstaff *et al.* (OPAL Collaboration), E. Phys. J. **C5**, 229 (1998).
- [12] D. S. Crowcroft, Ph.D. Thesis (Cornell University) 1998; also available as [http://w4.lns.cornell.edu/public/CLE0/analysis/tau/postscript/nutau\\_4pi.ps](http://w4.lns.cornell.edu/public/CLE0/analysis/tau/postscript/nutau_4pi.ps).
- [13] D. M. Asner *et al.* (CLEO Collaboration), Cornell preprint CLNS 99/1601, CLEO 99-01, submitted to Phys. Rev. D.
- [14] P. Abreu *et al.* (DELPHI Collaboration), Phys. Lett. B **426**, 411 (1998).